

Electron energy and electric field estimates in sprites derived from ionized and neutral N_2 emissions

J. Morrill,¹ E. Bucsele,² C. Siefiring,³ M. Heavner,⁴ S. Berg,⁵ D. Moudry,⁶ S. Slinker,³ R. Fernsler,³ E. Wescott,⁶ D. Sentman,⁶ and D. Osborne⁶

Received 31 August 2001; revised 22 March 2002; accepted 22 March 2002; published XX Month 2002.

[1] During the EXL98 aircraft mission, sprites and blue jets were observed by narrow band cameras that measure the N_2^+ 1NG (0,1) band at 4278Å and the N_2 2PG (0,0) band at 3370Å. We discuss the observations (~ 1 km resolution), instrumental and atmospheric corrections, and altitude profiles of ionized (1NG) and neutral (2PG) emission observed during a specific sprite. The ratio of ionized-to-neutral emission indicates a relative enhancement of ion emission below 55 km. Characteristic electron energies (E_{Ch}) and electric fields (E) are derived from these emission ratios using excitation rates computed from a model that solves the Boltzmann equation as a function of electric field. Up to 55km E follows the breakdown field (E_k) and E_{Ch} is ~ 2.2 eV. Above 55 km E drops below E_k and E_{Ch} drops to ~ 1.75 eV near 60km. *INDEX TERMS*: 0342 Atmospheric Composition and Structure: Middle atmosphere—energy deposition; 3304 Meteorology and Atmospheric Dynamics: Atmospheric electricity; 3324 Meteorology and Atmospheric Dynamics: Lightning; 3334 Meteorology and Atmospheric Dynamics: Middle atmosphere dynamics (0341, 0342)

1. Introduction

[2] The EXL98 Aircraft Campaign was a NASA sponsored mission to observe sprites and related phenomena from aircraft during July of 1998. A major goal was to measure neutral and ionized molecular nitrogen emission to examine ionization in sprites. The primary instrument configuration included narrow-band imagers that made video observations of the N_2^+ 1NG (0,1) band at 4278 and N_2 2PG (0,0) band at 3370Å. These imagers were provided by the Naval Research Laboratory and the University of Alaska Fairbanks, respectively. Other EXL98 observations measured UV sprite spectra [Heavner *et al.*, 2000]. Both observations are affected by atmospheric attenuation [Morrill *et al.*, 1998], and the EXL98 mission minimized this effect by using an aircraft as a high altitude observing platform.

[3] Spectral analysis studies indicate the presence of N_2^+ Meinel emissions in sprites [Green *et al.*, 1996; Morrill *et al.*, 1998]. These identifications involve relatively weak signals, as expected given N_2^+ (A) quenching [Piper *et al.*, 1985]. Green *et al.* [1996] compare model results with sprite spectra and estimate electron energies near 1 eV. Model estimates of blue and near-UV sprite emissions of N_2^+ and N_2 as well as electron energetics in sprites are presented by

¹E. O Hulburt Center for Space Research, Naval Research Laboratory, Washington, DC, USA.

²Goddard Earth Science and Technology Center, Baltimore, MD, USA.

³Plasma Physics Division, Naval Research Laboratory, Washington DC, USA.

⁴Los Alamos National Laboratory, Los Alamos, NM, USA.

⁵Computational Physics Inc., Springfield, VA, USA.

⁶Geophysical Institute, University of Alaska Fairbanks, Fairbanks, AL, USA.

numerous groups [Fernsler and Rowland, 1996; Pasko *et al.*, 1997; Rowland, 1998].

[4] Photometric observations of N_2^+ and N_2 in the blue and UV have been made from the ground [Armstrong *et al.*, 1998; Suszcynsky *et al.*, 1998; Armstrong *et al.*, 2000] hereafter (I, II, III). These studies produce precise time histories of sprite emissions with photometers. However, they integrate over a range of altitudes so variations in the time history with altitude were not determined. Initial work (I, II) used wide filter passbands that allowed both ionized (1NG) and neutral (2PG) emission into each channel and required extensive spectral modeling. Later work (III) used smaller passbands but still integrated over 15–25 km. The present observations integrate the sprite emission over 33 ms so that temporal information is limited. However, aircraft-based imaging and narrow-band filters provide altitude resolved profiles of the 1NG and 2PG emission with resolution improved over previous studies.

[5] In this paper we discuss the narrow-band EXL98 observations and the instrumental and atmospheric corrections used in the analysis. The resulting ratios of N_2^+ 1NG (0,1) to N_2 2PG (0,0) emission yield excitation rate ratios of N_2^+ (B) to N_2 (C). Characteristic electron energy (E_{Ch}) and electric field (E) estimates come from a comparison of the observed excitation rates with rates determined from a model that solves the Boltzmann equation as a function of electric field.

2. Observations

[6] Two sprites were observed at ~ 0900 UT on July 19, 1998, over Wisconsin. These sprites were observed from a single location so altitude and range information is based on the location of the two associated lightning strokes and known sprite morphology. Figure 1a shows the image from a broadband camera. Range to the sprite is ~ 360 km and the aircraft altitude was 14 km.

[7] Figure 1a also shows the field-of-view (FOV) of the 1NG and 2PG filtered cameras (inserted box). Figures 1b and 1c show the emission of the 1NG (0,1) and 2PG (0,0), respectively. The broadband image is saturated and not useful for this analysis. The central wavelengths and FWHM band-widths for these filters are 4282(14)Å and 3410(72)Å, respectively. The 2PG (0,0) is in the blue wing of the 3410Å filter. The two possible contaminating bands are the 2PG (1,5) and (4,5) bands in the 4282 and 3410Å passbands, respectively. Given filter rejection and intensity estimates, neither band produces a significant signal. 1NG observations used a Dage/MTI SIT VE1000 camera with a Fuji f/0.7 lens. 2PG observations used a GEN IIUV V53-1845 Video Scope camera and a Lyman Alpha II f/1.7 lens. This analysis focuses on the left sprite in Figure 1a.

3. Analysis and Results

[8] These observations require a number of corrections. The 2PG image is scaled to the 1NG image. Figures 1b and 1c show three narrow vertical regions with the left sprite in the central region. The two outer regions provide the background. The central region is summed horizontally and the residual sprite emission is the difference between the smoothed fits to the sprite and back-

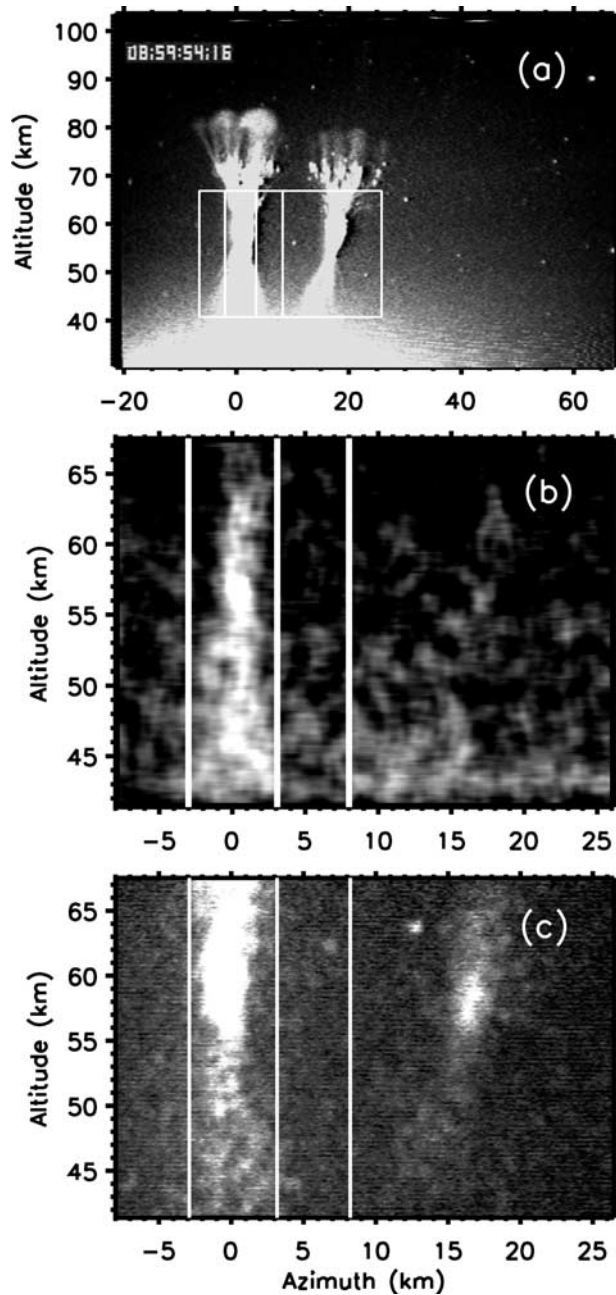


Figure 1. Image of sprites from (a) broad-band camera, (b) 1NG filtered camera (c) 2PG filtered camera.

ground profiles. The 1NG and 2PG profiles are in Figure 2 and have ~ 1 km altitude resolution.

[9] Other instrumental and atmospheric corrections are applied to these profiles. Corrections account for the peak wavelength (angle dependent) and spectral shape of the passband filters, camera flat field, absolute calibration and altitude-dependent atmospheric attenuation (MOSART atmospheric transmission model [Morrill *et al.*, 1998]). All corrections are slowly varying with altitude so large changes in the intensity profiles cannot be attributed to instrumental or atmospheric effects.

[10] Figure 3 shows the corrected intensity profiles for the ionized (1NG) and neutral (2PG) emissions. The 1NG emission remains roughly constant at all altitudes with a slight increase at lower altitudes. The 2PG profile is brighter and more structured than the 1NG profile. Above 55 km the neutral emission dominates

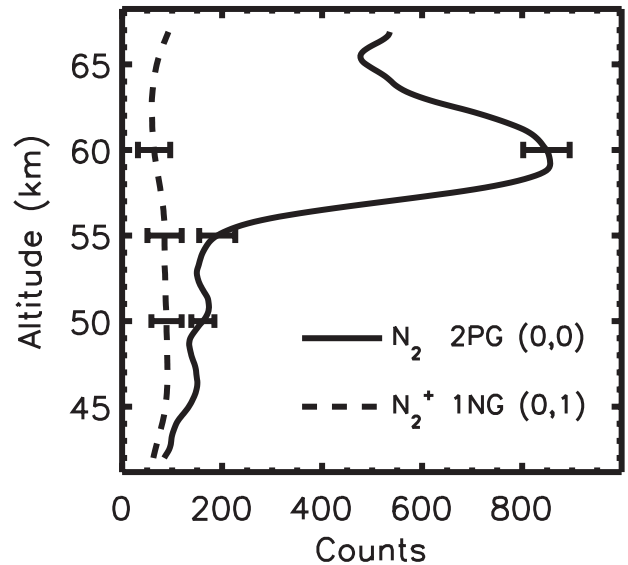


Figure 2. Residual sprite emission profiles for the 1NG (0, 1) and 2PG (0, 0) band emissions.

and varies significantly while below 55 km it is roughly constant. The ratio of these emissions appears in Figure 4 and shows two regions; the upper portion or “body” and the lower portion or “tendrils.” These results indicate a relative enhancement in ionization in the tendrils.

[11] A number of assumptions allow E_{Ch} and E to be estimated from the intensity ratios. The intensity is

$$I_{v'v''} = k_e N_2 n_e A_{v'v''} q / \left(1 / \tau_{v'} + k_q^{N_2} N_2 + k_q^{O_2} O_2 \right) \quad (1)$$

with k_e the excitation coefficient, N_2 and n_e the nitrogen and electron densities, $A_{v'v''}$ the transition probability, q the Franck-Condon factor, $\tau_{v'}$ the lifetime, and k_q the quenching coefficients (see Table 1).

[12] Equation (1) applies to the instantaneous intensities, but our emission data are time-integrated. To allow for this difference we assume: a sprite consists of waves of ionization (i.e., streamers);

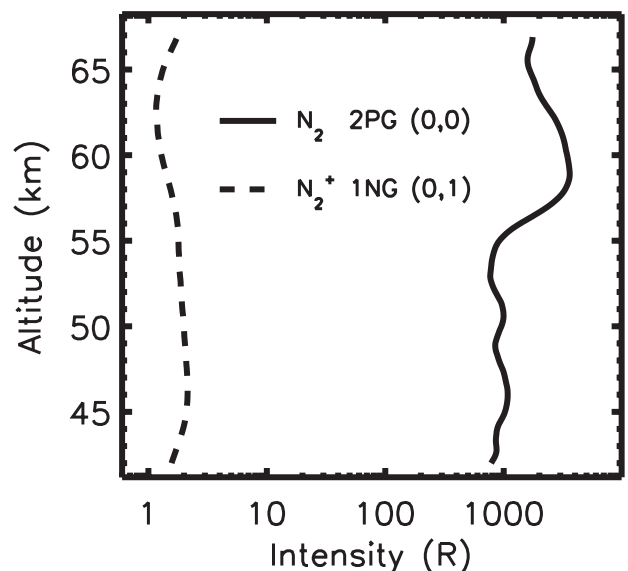


Figure 3. 1NG (0, 1) and 2PG (0, 0) intensity profiles.

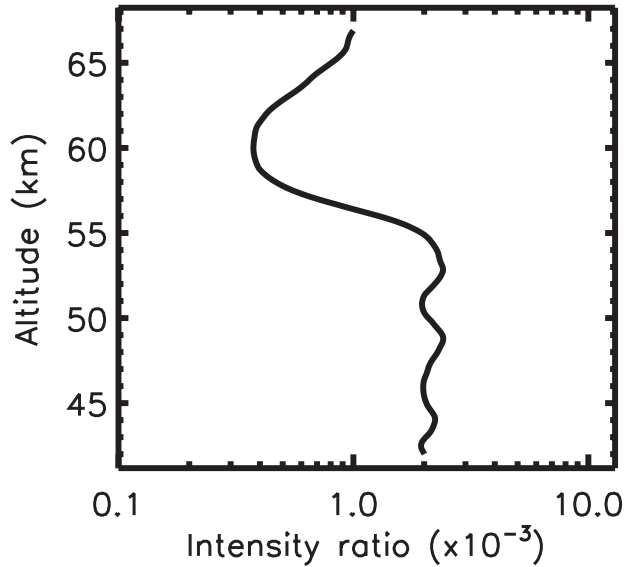


Figure 4. 1NG (0, 1)/2PG (0, 0) intensity ratios.

E_{Ch} is determined by the instantaneous electric field E ; E_{Ch} is small compared with the threshold excitation energies of the 1NG and 2PG upper states (~ 10 – 20 eV). In this case, k_e is a strong function of E . Ahead of the streamer E and k_e are large while n_e is small. In the streamer head E and k_e are large with n_e increasing. Finally, in the streamer body E and k_e are small while n_e is large [Raizer *et al.*, 1998]. Thus, I_{ν} peaks in the streamer head where both k_e and n_e are large. For the case where the emission peaks near the streamer head and persists for less time than for the streamer to cross one pixel ($\Delta h \sim 1$ km) [Stanley *et al.*, 1999], the ratio of the peak intensities is approximately the ratio of the time-integrated emissions. We then estimate E_{Ch} and E in the streamer head as a function of altitude using equation (1), the measured intensity ratio, and the results of a Boltzmann code [Slinker *et al.*, 1990] run with 20% O_2 /80% N_2 .

[13] For the model to apply, Δh should be small compared with the neutral scale height (~ 10 km) but large compared with the ionization front (~ 0.1 km [Gerken *et al.*, 2000]). The latter assumption is best met at low altitude, since the width of the front varies inversely with density. If the assumption fails, the model underestimates the values of E_{Ch} and E in the streamer head, because the lower excitation energy of the 2PG upper state allows its emission to persist (III). The results from this model appear in Figure 5. Errors in E_{Ch} are ~ 0.1 eV and reflect intensity uncertainties.

4. Discussion

[14] Sprite processes require observations at small spatial, spectral, and temporal scales. So far, no single study has simultaneously probed all three scales. Photometric studies of N_2^+ and N_2 emissions (I, II, III) yield detailed time history but little spatial information. High speed video [Stanley *et al.*, 1999] yields spatial and temporal results but little spectral data. The current results give

Table 1. Radiative and Kinetic Parameters

Parameter	$N_2(C)$	$N_2^+(B)$
$\tau(s)$	3.71×10^{-8}	6.23×10^{-8}
$A(s^{-1})$	1.31×10^7	3.71×10^6
q	5.45×10^{-1}	8.83×10^{-1}
$k_q^{O_2}(cc/s)$	5.48×10^{-10}	6.20×10^{-10}
$k_q^{N_2}(cc/s)$	3.59×10^{-11}	7.50×10^{-11}

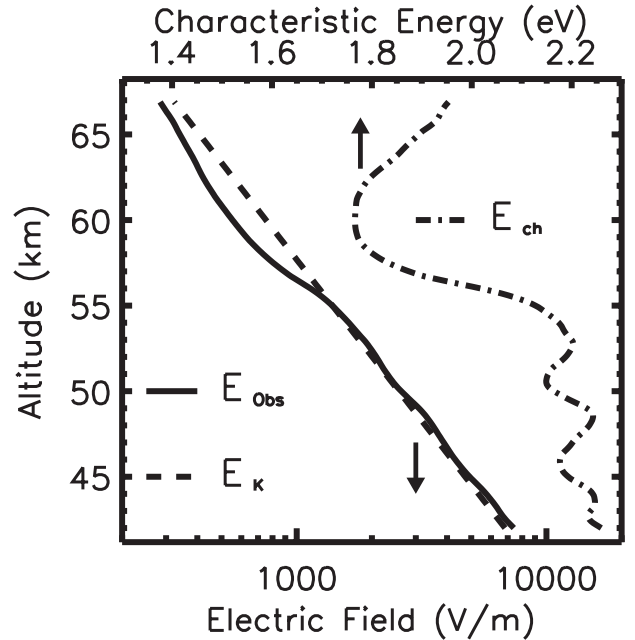


Figure 5. Electric field (E) and electron energy (E_{Ch}) from intensities as well as breakdown field (E_k).

limited temporal information but yield spatial (altitude) and spectral information. Given the differing 1NG and 2PG emission profiles, neither photometry nor high-speed video can resolve issues of sprite energetics without considering the present results.

[15] The present analysis is valid when the emission ratio is constant in time or dominated by one value. This should be valid for a propagating streamer breakdown, since 1NG/2PG emission intensity is weighted to times where E_{Ch} and n_e are large. The 1NG/2PG intensity ratio (Figure 4) shows two distinct regions, above and below 55 km. E_{Ch} in Figure 5 decreases with decreasing altitude to ~ 60 km. A transition occurs between 60–55 km with the E_{Ch} increasing to ~ 2.2 eV below 55 km. Maxwell-Boltzmann (MB) distributions do not accurately yield E_{Ch} in sprites, but for comparison, MB temperatures are ~ 0.8 times E_{Ch} in Figure 5.

[16] We interpret our results in light of high speed video observations [D Moudry, private comm.] that show “tendrils” emissions occur for ~ 1 ms while “body” emissions continues for ~ 10 ms. This is consistent with ionization occurring during an initial hot phase (~ 1 ms) (I, II, III) at 40–70 km with a longer cool phase above 55 km where neutral emission dominates. Below 55 km, one interpretation is that emissions are from the ionizing portion of the streamer tip and so indicate the electric field is capped at the breakdown field. As a result, E_{Ch} values below 55 km are the characteristic electron energies during ionization. Above 55 km, the measured E_{Ch} are upper bounds for E_{Ch} during the cooler phase.

5. Conclusion

[17] Analysis of narrow passband sprite observations of 1NG and 2PG emissions yield estimates of E_{Ch} and E as a function of altitude, using a Boltzmann model. The results show the electric field follows the local breakdown field, E_k , at altitudes below 55 km with $E_{Ch} \sim 2.2$ eV. Above 55 km, 2PG emission is ~ 5 X above that at lower altitudes, the derived field is $\sim 30\%$ below E_k , and E_{Ch} reaches a minimum of ~ 1.75 eV at 60 km. The latter field values are below E_k since the model underestimates the peak E and E_{Ch} during ionization at low gas density. Above 55 km, measured E_{Ch} represents the upper bound to E_{Ch} during the cooler phase after ionization. These results indicate that most emission in sprites

results from classical gas breakdown followed, at higher altitudes, by an afterglow with lower E_{Ch} . This method shows promise for providing time varying E_{Ch} in sprites when coupled with a dynamic streamer model and spatial, spectral, and temporally resolved data.

[18] **Acknowledgments.** The EXL98 project was supported by NASA Grants NAG5-5019 and NAG5-5172, Office of Naval Research 6.1 research funds, and the Space Vehicles Directorate of the Air Force Research Laboratory.

References

- Armstrong, R., J. Shorter, M. Taylor, D. Susczynsky, W. Lyons, and L. Jeong, Photometric measurements in the SPRITES 1995 and 1995 campaigns, *J. Atmos. Sol. Terr. Phys.*, *60*, 787–799, 1998.
- Armstrong, R., D. Susczynsky, W. Lyons, and T. Nelson, Multi-color photometric measurements of ionization and energy in sprites, *Geophys. Res. Lett.*, *27*, 653–656, 2000.
- Fernsler, R., and H. Rowland, Models of lightning-produced sprites and elves, *J. Geophys. Res.*, *101*, 29,653–29,656, 1996.
- Green, B., M. Fraser, W. Rawlins, L. Jeong, W. Blumberg, S. Mende, G. Swenson, D. Hampton, E. Wescott, and D. Sentman, Molecular excitation in sprites, *Geophys. Res. Lett.*, *23*, 2161–2164, 1996.
- Gerken, E., U. Inan, and C. Barrington-Leigh, Telescopic imaging of sprites, *Geophys. Res. Lett.*, *27*, 2637–2640, 2000.
- Heavner, M., D. Sentman, D. Moudry, E. Wescott, C. Siefing, J. Morrill, and E. Bucsel, Sprites, Blue Jets, and Elves: Optical evidence of energy transport across the Stratopause, in *Atmospheric Science Across the Stratopause*, edited by D. E. Siskind, S. D. Eckerman, and M. E. Summers, pp. 69–82, American Geophysical Union, Washington, DC, 2000.
- Morrill, J., and W. Benesch, Auroral N_2 emissions and the effect of collisional processes on the N_2 triplet state vibrational populations, *J. Geophys. Res.*, *101*, 261–274, 1996.
- Morrill, J., E. Bucsel, V. Pasko, S. Berg, M. Heavner, D. Moudry, W. Benesch, E. Wescott, and D. Sentman, Time resolved N_2 triplet state vibrational populations and emissions associated with red sprites, *J. Atmos. Sol. Terr. Phys.*, *60*, 811–829, 1998.
- Pasko, V., U. Inan, T. Bell, and Y. Taranenko, Sprites produced by quasi-electrostatic heating and ionization in the lower ionosphere, *J. Geophys. Res.*, *102*, 4529–4561, 1997.
- Pasko, V., U. Inan, and T. Bell, Spatial structure of sprites, *Geophys. Res. Lett.*, *25*, 2123–2126, 1998.
- Piper, L., B. Green, W. Blumberg, and S. Wolnik, N_2^+ Meinel band quenching, *J. Chem. Phys.*, *82*, 3139–3145, 1985.
- Raizer, Y., G. Milikh, M. Sheider, and S. Novakovski, Long streamers in the upper atmosphere above thunderclouds, *J. Phys. D: Appl. Phys.*, *31*, 3255–3264, 1998.
- Rowland, H., Theories and simulations of elves, sprites, and blue jets, *J. Atmos. Sol. Terr. Phys.*, *60*, 831–844, 1998.
- Slinker, S., A. Ali, and R. Taylor, High-energy electron beam deposition and plasma velocity distribution in partially ionized N_2 , *J. Appl. Phys.*, *67*, 679–690, 1990.
- Stanley, M., P. Krehbiel, M. Brook, C. Moore, and W. Rison, High speed video of initial sprite development, *Geophys. Res. Lett.*, *26*, 3201–3204, 1999.
- Susczynsky, D., R. Roussel-Dupre, W. Lyons, and R. Armstrong, Blue-light imagery and photometry of sprites, *J. Atmos. Sol. Terr. Phys.*, *60*, 801–809, 1998.
-
- J. Morrill, C. Siefing, S. Slinker, and R. Fernsler, Naval Research Laboratory, Washington, DC 20375, USA.
- E. Bucsel, NASA/GSFC, Code 916 Greenbelt, MD 20771, USA.
- M. Heavner, NIS-1, Los Alamos National Laboratory Los Alamos, NM 87545, USA.
- S. Berg, Computational Physics, Inc. Springfield, VA 22151, USA.
- D. Moudry, D. Osborne, D. Sentman, and E. Wescott, Geophysical Institute, University of Alaska Fairbanks, Fairbanks AK 99775, USA.